Journal of Neuroscience Research

Journal of Neuroscience Research 89:650–660 (2011)

Cilostazol Enhances Integrin-Dependent Homing of Progenitor Cells by Activation of cAMP-Dependent Protein Kinase in Synergy With Epac1

Dong Hyung Lee, Hye Rin Lee, Hwa Kyoung Shin, So Youn Park, Ki Whan Hong, Eun Kyoung Kim, Sun Sik Bae, Won Suk Lee, Byung Yong Rhim, and Chi Dae Kim*

Medical Research Center for Ischemic Tissue Regeneration, Department of Pharmacology, School of Medicine, Division of Meridian and Structural Medicine, Department of Obstetrics and Gynecology, Pusan National University, Beomeo-ri, Mulgeum-eup, Yangsan-si, Gyeongsangnam-do, Korea

Recruitment and adhesion of exogenous endothelial progenitor cells (EPCs) or endogenously mobilized bone marrow mononuclear cells (BM MNCs) to the sites of ischemia is an important focus of cell therapy. This study sought to determine whether cilostazol enhances integrin-dependent homing of progenitor cells both in vitro and in vivo. In the in vitro experiments with human umbilical cord blood (HUCB)-derived EPCs, cilostazol (10 μM) stimulated up-regulation of integrins β1, α1, and αv as well as 8-pCPT-2′-O-Me-cAMP (100 μM; 8-pCPT, Epac activator). Cilostazol and 8-pCPT significantly enhanced migration and adhesion of HUCB EPCs to a fibronectin-coated plate and endothelial cells, which were inhibited by KT5720 (PKA inhibitor, 1 μM) and GGTI-298 (Rap1 inhibitor, 20 μM). Cilostazol stimulated Epac1 expression and up-regulated the active Rap1, as did 8-pCPT, and they were suppressed by KT5720 ($P < 0.001$) and GGTI-298 ($P < 0.001$). 8-pCPT increased p-CREB expression and stimulated PKA activity, which was inhibited by KT5720, Rp-cAMPS, and GGTI-298. In addition, N^6-benzoyl-cAMP (100 μM) increased Rap1 GTP expression, as did 8-pCPT; they were suppressed by Rp-cAMPS and GGTI-298. The in vivo experiments showed that cilostazol (30 mg/kg/day, orally for 7 days) significantly enhanced the integrin β1 expression in the molecular layer and up-regulated homing of BM MNCs to the injured molecular layer with increased capillary density in mouse brain subjected to transient forebrain ischemia ($n = 6$, $P < 0.001$). In conclusion, cilostazol stimulated integrin expression and enhanced migration and adhesion of progenitor cells through cooperative activation of PKA and Epac signals; such activity may improve the efficacy of cell therapy for ischemic disease.

Key words: EPC; Epac1; Rap1; integrin; PKA

Modulation of cardiovascular function by circulating premature cells derived from bone marrow, known as endothelial progenitor cells (EPCs), has been demonstrated to promote vascular repair and enhance neovascularization in ischemic organs (Asahara et al., 1997). The major step in the recruitment of EPCs to ischemic tissue is adhesion and transmigration of progenitor cells to endothelial cell layers (Vajkoczy et al., 2003; Urbich and Dimmeler, 2004). Integrins mediate cell–cell or cell–matrix adhesion and are involved in the homing of EPCs to sites of active neovascularization (Wu et al., 2006; Jin et al., 2006). In particular, integrin β1, a cell adhesion molecule, is the principal endothelial receptor for basal lamina components, such as collagen and laminin and, thus, contributes to cerebral microvascular integrity (Burggraf et al., 2008).

Cilostazol (6-[4-(1-cyclohexyl-1H-tetrazol-5-yl)-butoxy]-3,4-dihydro-2-(1H)-quinolinone) increases intracellular cAMP levels through inhibition of type III phosphodiesterase (Kimura et al., 1985). Cilostazol has been shown to exert protective effects against transient focal cerebral ischemia and chronic cerebral hypoperfusion injury by decreasing ischemic brain infarction by

Additional Supporting Information may be found in the online version of this article.

D.H. Lee and H.R. Lee contributed equally to this work.

Contract grant sponsor: MRC Program; Contract grant number: 2010-0001245; Contract grant sponsor: Basic Science Research Program through the National Research Foundation of Korea (NRF) funded by the Ministry of Education, Science and Technology; Contract grant number: 2009-0066654.

*Correspondence to: Chi Dae Kim, Department of Pharmacology, School of Medicine, Pusan National University, Yangsan-si, Gyeongsangnam-do 626-870, Republic of Korea. E-mail: chidkim@pusan.ac.kr

Received 4 June 2010; Revised 25 October 2010; Accepted 25 October 2010

Published online 17 February 2011 in Wiley Online Library (wileyonlinelibrary.com). DOI: 10.1002/jnr.22558

inhibition of apoptotic and oxidative cell death (Lee et al., 2008). Recently, Shin et al. (2010) reported that cilostazol increases Sca-1/vascular endothelial growth factor receptor 2-positive cells in the bone marrow and circulating blood, associated with an increased number of stromal cell-derived factor-1α-positive cells in the molecular layer of the hippocampus that colocalized with CD31 in a mouse model of transient forebrain ischemia. These findings suggest that cilostazol increased recruitment of bone marrow-derived (BM) stem cells to areas of injured tissues.

Epac (exchange protein directly activated by cAMP) was introduced as a novel cAMP-dependent but PKA-independent guanine nucleotide-exchange factor for the small G-protein Rap (de Rooij et al., 1998; Kawasaki et al., 1998). The Epac protein is a novel cAMP sensor that regulates several pivotal cellular processes, including cell proliferation, cell differentiation, and cell–cell adhesion events (Roscioni et al., 2008). Evidence has emerged showing that Rap1 activates integrin activity and regulates integrin- and cadherin-dependent adhesion in many cellular systems (Bos, 2005; Kooistra et al., 2007). Carmona et al. (2008) reported that stimulation of Epac1 by 8-pCPT activated β1- and β2-integrins in EPC and increased integrin-dependent activity, such as adhesion and migration in vitro, and enhanced homing of intravenously injected EPC to the ischemic limbs in a murine model of hind limb ischemia. Lorenowicz et al. (2008) demonstrated that both PKA and Epac1 pathways require integrin engagement to stimulate endothelial cell migration. Although PKA and Epac have been shown to act independently, the relative contribution and potential cross-talk between these two pathways, with regard to adhesion and migration of EPCs, have not been determined.

EPCs can be isolated from bone marrow, human cord blood, and peripheral blood. Murohara (2001) initially reported on the utility of human umbilical cord blood-derived EPCs; HUCB EPCs, as abundant EPCs, can be isolated from a relatively small volume of cord blood. The transplantation of EPCs has been shown to augment neovascularization effectively in response to hindlimb ischemia (Carmona et al., 2008).

In this study, in vitro and in vivo experiments were performed. For the in vitro study, investigation of whether cilostazol 1) stimulates expression of integrins and 2) promotes transendothelial migration/adhesion was evaluated, and 3) the mechanism(s) by which cilostazol modulates integrin-dependent migration and adhesion by regulation of the cAMP-dependent PKA and Epac1-Rap1 signal pathways was studied. For the in vivo experiment, cilostazol-stimulated enhanced recruitment of intravenously injected MNCs, isolated from mouse bone marrow, to capillary endothelial cells, and the increased capillary density, a marker of neovasculogenesis, in the hippocampal CA1 ischemic area, were studied in a mouse model of transient forebrain ischemia.

MATERIALS AND METHODS

Isolation and Cultivation of EPCs

HUCB samples (about 50 ml each) were collected by gravity flow from fresh placentas with attached umbilical cords from mothers that had undergone normal delivery without concomitant disease. The Institutional Review Board at the Pusan National University School of Medicine approved all protocols, and informed consent was obtained from all adult donors and parents of newborns. Mononuclear cells were isolated from HUCB by density gradient centrifugation using 1.077 g/liter Ficoll-paque (GE Healthcare, Piscataway, NJ) as described previously (Asahara et al., 1997). The mononuclear cells (1×10^7) were plated in endothelial growth medium (EGM-2 MV Bullet Kit system; Cambrex, Taufkirchen, Germany) with heparin on 2% gelatin-coated six-well plates and incubated in a 5% CO_2 incubator at 37°C.

Bone marrow was isolated from the tibias and femurs of C57BL/6 mice at 5–7 weeks of age. The bone marrow was passed through a 40-μm nylon mesh cell strainer (BD Falcon, Oxnard, CA). The bone marrow cells were isolated by Ficoll-Histopaque 1083 (Sigma, St. Louis, MO) separating medium for 30 min at 2,500 rpm and were washed twice in phosphate-buffered saline (PBS); thereafter, the cells (1×10^7) were plated in endothelial growth medium (EGM-2 MV Bullet Kit system) on 1.5% gelatin-coated six-well plates, and incubated in a 5% CO_2 incubator at 37°C.

On day 7 of culture, adherent cord blood EPCs were harvested in phosphate-buffered solution and incubated for 4 hr with fluorescent dye, 2.6 μg/ml 1,1′-dioctadecyl-3,3,3′,3′-tetramethylindocarbocyanine-labeled DiI-acLDL (Molecule Probes, Eugene, OR) at 37°C. Thereafter, the cultures were washed, fixed with 1% formaldehyde for 10 min, and washed again with PBS. Fluorescein isothiocyanate-labeled lectin from *Ulex europaeus* agglutinin, 10 μg/ml (UEA-1; Sigma), was added at a concentration of 10 μg/ml and incubated for 1 hr at 25°C. Human brain microvascular endothelial cells (HBMECs) were purchased from the Applied Cell Biology Research Institute (Kirkland, WA) and cultured using the EGM-2 MV Bullet Kit system (Cambrex).

Western Blot Analysis

After stimulation with cilostazol and 8-pCPT (15 min), the EPCs were scraped using an ice-cold lysis buffer. After centrifugation at 12,000 rpm, 30 μg of total proteins from each sample was loaded into a 10% SDS-polyacrylamide gel, and separated proteins were transferred to a nitrocellulose membrane (Amersham Biosciences, Piscataway, NJ). The membrane was blocked with 5% skim milk, followed by incubation with a 1:1,000 dilution of anti-Epac1 (Abcam, Cambridge, United Kingdom), anti-human integrin β1, anti-human integrin αV (Santa Cruz Biotechnology, Santa Cruz, CA), and anti-human integrin α1 (Millipore, Bedford, MA) in 5% bovine serum albumin in phosphate-buffered saline at 4°C overnight. After incubation of blots with IgG horseradish peroxidase-conjugated secondary antibody, the intensity of the chemiluminescence was measured using a Fluorochem gel image analyzer (MF-Chem Bis 3.2; Alpha Innotech,

San Leandro, CA). The membrane was reprobed with an anti-β-actin antibody (MP Biomedicals, Aurora, OH) as an internal control.

Rap1 Activity Assay

To examine whether stimulation of Epac1 by cilostazol would increase the active GTP-bound form of Rap1 in the EPCs, the levels of activated Rap1 were determined by pull-down assays with a glutathione S-transferase (GST) fusion protein containing the Rap1 binding domain (RBD) of human RalGDS for affinity precipitation of active Rap1 (GTP-Rap1) from cell lysates (Rangarajan et al., 2003). Human RalGDS-RBD was kindly provided by Dr. J.L. Bos (University Medical Center Utrecht, Utrecht, Netherlands). After treatment with cilostazol for 15 min, the cells were lysed, and 0.5 ml of cleared lysate was incubated with 50 μg GST-RalGDS-RBD bound to glutathione beads. After rotation for 90 min at 4°C, beads were washed four times and boiled in sample buffer. The samples were separated by 10% SDS-PAGE, blotted to a nitrocellulose membrane, probed with anti-Rap1 antibody (Stressgen, Ann Arbor, MI), and visualized by enhanced chemiluminescence (Amersham Biosciences).

Protein Kinase A Activity Assay

The effects of cilostazol and 8-pCPT on PKA activity were assessed in the lysate of HUCB EPCs using a PKA kinase activity kit (Enzo Life Sciences, Warrington, PA) according to the manufacturer's instructions. Briefly, the wells of the PKA microtiter plate were soaked with 50 μl kinase assay dilution buffer at room temperature for 10 min. The samples were added to the wells of a PKA substrate microtiter plate. Reaction was initiated by addition of 10 μl of diluted ATP to each well, except for the blank well, and incubated for up to 90 min at 30°C. Then, 40 μl of phosphor-specific substrate antibody was added to each well and incubated at room temperature for 60 min. After washing, 40 μl of diluted anti-rabbit IgG:HRP conjugate was added to each well for 30 min, followed by exposure to the tetramethylbenzidine substrate (for 30–60 min); the reaction was then stopped. Absorbance at 450 nm was determined using a microplate reader (Molecular Devices, Sunnyvale, CA).

Transmigration of EPCs

To assess the effects of cilostazol and 8-pCPT-2′-O-Me-cAMP on transcellular migration of EPCs, cells were grown and serum-starved for 6 hr prior to plating in a ChemoTx chamber (Neuro Probe, Gainthersburg, MD; Vasa et al., 2001). For the migration assay, the bottom side of the ChemoTx membrane was coated with gelatin at 4°C overnight, and a total of 1×10^5 serum-starved cells in a 50 μl volume was placed on the top side of the ChemoTx membrane. After fixation, the ChemoTx membrane was stained with DAPI, and the migrated cells were counted using a fluorescence microscope at 10× magnification (Axio Imager M1 high-quality fluorescence microscope; Carl Zeiss, Oberkochen, Germany).

Transient Forebrain Ischemia

As reported previously (Shin et al., 2010), all procedures were conducted in accordance with the animal care guidelines of the Animal Experimental Committee of Pusan National University. Male C57BL/6 mice (Samtako BioKorea, Korea) weighing 20–25 g were anesthetized with 1.5% isoflurane (in 70% N_2O and 30% O_2). Both common carotid arteries were carefully separated from the vagus nerve and occluded for 20 min with microclips. For reperfusion, the clips were removed. Then, 100 μl of CM-DiI (Molecular Probes)-labeled BM MNCs suspension (1×10^6 cells) was injected via the tail vein 48 hr after ischemia. Animals received cilostazol (30 mg/kg/day, 100 μl orally) or vehicle (30% DMSO, 100 μl) for 1 hr by means of oral gavage after surgery and afterward once daily for 7 and 14 days. The endothelial cell density was determined by staining of von Willebrand factor (vWF), a specific marker for endothelial cells.

Tissue Preparation and Immunofluorescence

Seven days after the forebrain ischemic insult, the mice were deeply anesthetized with thiopental sodium and perfused transcardially with PBS. The brains were frozen and stored at −70°C. Ten-micrometer-thick sections were cut serially on a cryostat. The sections were incubated with blocking solution (CAS Block; Zymed Laboratories, South San Francisco, CA) for 10 min and then overnight with a 1:100 dilution of antiintegrin β1 antibody (Santa Cruz Biotechnology) and anti-von Willebrand factor (vWF; Dako, Glostrup, Denmark). After washing, the sections were incubated with a 1:100 dilution of secondary antibody solution containing fluorescein anti-rabbit IgG (Vector Laboratories, Burlingame, CA) for 1 hr at room temperature. An Axio Imager M1 high-quality fluorescence microscope (Carl Zeiss) was used for detection of fluorescence.

Drugs

Cilostazol [OPC-13013, 6-[4-(1-cyclohexyl-1*H*-tetrazol-5-yl) butoxy]-3,4-dihydro-2-(1*H*)-quinolinone] was donated by Otsuka Pharmaceutical Co. Ltd. (Tokushima, Japan) and dissolved in dimethyl sulfoxide as a 10 mM stock solution. The 8-(4-chloro-phenylthio)-2′-*O*-methyladenosine-3′,5′-cyclic monophosphate was purchased from Sigma-Aldrich and dissolved in distilled water (10 mM stock solution). KT5720 was obtained from Alexis Enzo Life Sciences, and GGTI-298 was from Calbiochem (San Diego, CA). Epac1 was purchased from Abcam (Cambridge, United Kingdom).

Statistical Analyses

Data are expressed as mean ± SEM. Comparison of changes in variable parameters between vehicle and cilostazol treatment groups without and with inhibitors was analyzed by one-way analysis of variance, followed by Tukey's multiple comparison tests as a post hoc comparison. Student's *t*-test was used to determine the difference in the means of the two groups. Statistical analysis was performed in Sigmastat software (Systat Software, Point Richmond, CA). A value of $P < 0.05$ was considered statistically significant.

RESULTS

Whether cilostazol could elevate intracellular cAMP levels as a phosphodiesterase type III inhibitor in the HUCB EPCs was evaluated. The HUCB-derived mononuclear cells cultured for 7 days were incubated with a vehicle (0.1% DMSO) or cilostazol (1–30 μM) for 15 min. The cell lysates showed that the intracellular cAMP levels were significantly increased by cilostazol (1, 3, 10, and 30 μM) in a concentration-dependent manner (Supp. Info. Fig. 1A).

In addition, cilostazol and Epac were studied to determine whether they could preserve intact HUCB EPCs. Treatment with either cilostazol (10 and 30 μM) or 8-pCPT (100 and 200 μM) significantly reduced the TNF-α (100 ng/ml)-induced increase of trypan blue-positive cells (Supp. Info. Fig. 1B).

Furthermore, whether cilostazol could improve proliferation of HUCB EPCs was studied. The MTT assay showed that, after treatment with cilostazol (1–10 μM) for 24 hr, cell counts showed an increase in cell proliferation in a concentration-dependent manner; this was significantly suppressed by KT 5720 (1 μM, $P < 0.001$), a selective inhibitor of PKA and GGTI-298 (20 μM, a Rap1 inhibitor; Supp. Info. Fig. 1C).

Enhancement of Tube Formation on the Matrigel and Colony Formation

The effect of cilostazol on HUCB EPC activity was assessed by measurement of in vitro tube and colony formation. After 7 days of culture, the cells showed evidence of enhanced differentiation, such as a cord-like structure. The effect of cilostazol on EPC activity was assessed by measurement of in vitro tube and colony formation. Treatment with cilostazol (1–30 μM) promoted formation of tubular network structures in a concentration-dependent manner; this was suppressed by KT5720 (1 μM) and GGTI-298 (20 μM; Supp. Info. Fig. 2A).

For assessment of the colony expansion potential, the HUCB EPCs were cultivated for 7 days in the presence or absence of cilostazol. The cells were then detached, and 1×10^6 HUCB EPCs were seeded onto methylcellulose plates. The colony size was significantly enhanced in the HUCB EPCs pretreated with cilostazol. Enhancement of the size of colony formation was significantly suppressed by KT5720 (1 μM) and GGTI-298 (20 μM; Supp. Info. Fig. 2B). Therefore, the results of this experiment suggest that cilostazol-activated PKA and Epac1/Rap1 signals were involved in the promotion of proliferation and preservation of the functions of HUCB EPC activity.

Increase in Integrin Expression of HUCB EPCs

The phenotype of ex-vivo-cultivated HUCB EPCs was confirmed by double-positive immunostaining with uptake of Dil-Ac-LDL and FITC-UEA-1 binding. Cellular immunostaining showed double-positive staining for uptake of Dil-ac-LDL and binding of FITC-UEA-l by most adherent cells (>90%). These findings indicated HUCB EPC characteristics (Fig. 1A).

To assess the role of PKA and Epac1 in integrin expression by cilostazol, whether Epac1 activation after exposure to cilostazol can affect the expression of β1-integrin in the HUCB EPCs was studied. Indeed, cilostazol (10 μM) induced up-regulation of integrin β1 (338.2% ± 13.5%, $P < 0.001$ vs. vehicle); this was significantly inhibited by both KT5720 (174.1% ± 16.9%, $P < 0.001$) and GGTI-298 (138.7% ± 14.8%, $P < 0.001$). Similarly, 8-pCPT (100 μM) significantly stimulated expression of the integrin β1, but less than cilostazol; the expression was inhibited by both KT5720 and GGTI-298 (Fig. 1B). Expression of integrin subunits α1 (Fig. 1C) and αv (Fig. 1D) was up-regulated by cilostazol and 8-pCPT and was significantly inhibited by KT5720 and GGTI-298, respectively (Fig. 1C,D).

Increased Transcellular Migration and Adhesion of HUCB EPCs

The effects of cilostazol and 8-pCPT on transcellular migration of the HUCB EPCs were assessed. Preincubation of the EPCs with cilostazol for 15 min resulted in a significant and concentration-dependent increase in their migration to the fibronectin-coated plate by up to 514% ± 15% with 30 μM cilostazol. Treatment with 8-pCPT was associated with up-regulation, with less of an effect (Fig. 2A). Cilostazol-stimulated migration (10 μM, 420.5% ± 29.8%) was significantly suppressed by both KT5720 (247.0% ± 9.3%, $P < 0.01$) and GGTI-298 (234.4% ± 17.1%, $P < 0.01$). The 8-pCPT treatment stimulated transcellular migration, similarly to cilostazol (Fig. 2B). These data suggest that activation of Epac1, as well as PKA, by cilostazol can increase the transcellular migratory capacity of HUCB EPCs in matrix proteins.

Two different adhesion assays were performed to determine the adhesiveness of the cultured HUCB EPCs. First, cilostazol and activation of Epac1 increased progenitor cell adhesion to fibronectin. The EPCs exposed to cilostazol for 15 min showed a significant increase in the number of adhesive cells (655.0% ± 22.5%, $P < 0.01$ by 10 μM cilostazol). In addition, 8-pCPT (100 μM) showed increased adhesion; however, the increase was less than that with cilostazol (Fig. 2C). Second, the number of cilostazol-treated EPCs incorporated into an HBMEC monolayer was determined. Preincubation of the HUCB EPCs with cilostazol (1–30 μM) resulted in a dose-dependent increase in the adhesion of the EPCs to matured HBMEC monolayers. This effect of the 10 μM cilostazol effect (2892.9% ± 247.1%) was suppressed by both KT5720 (242.9% ± 68.1%, $P < 0.01$) and GGTI-298 (100.0% ± 7.1%, $P < 0.01$; Fig. 2D). These findings suggest that cilostazol may enhance the adhesiveness of EPCs to ischemic sites.

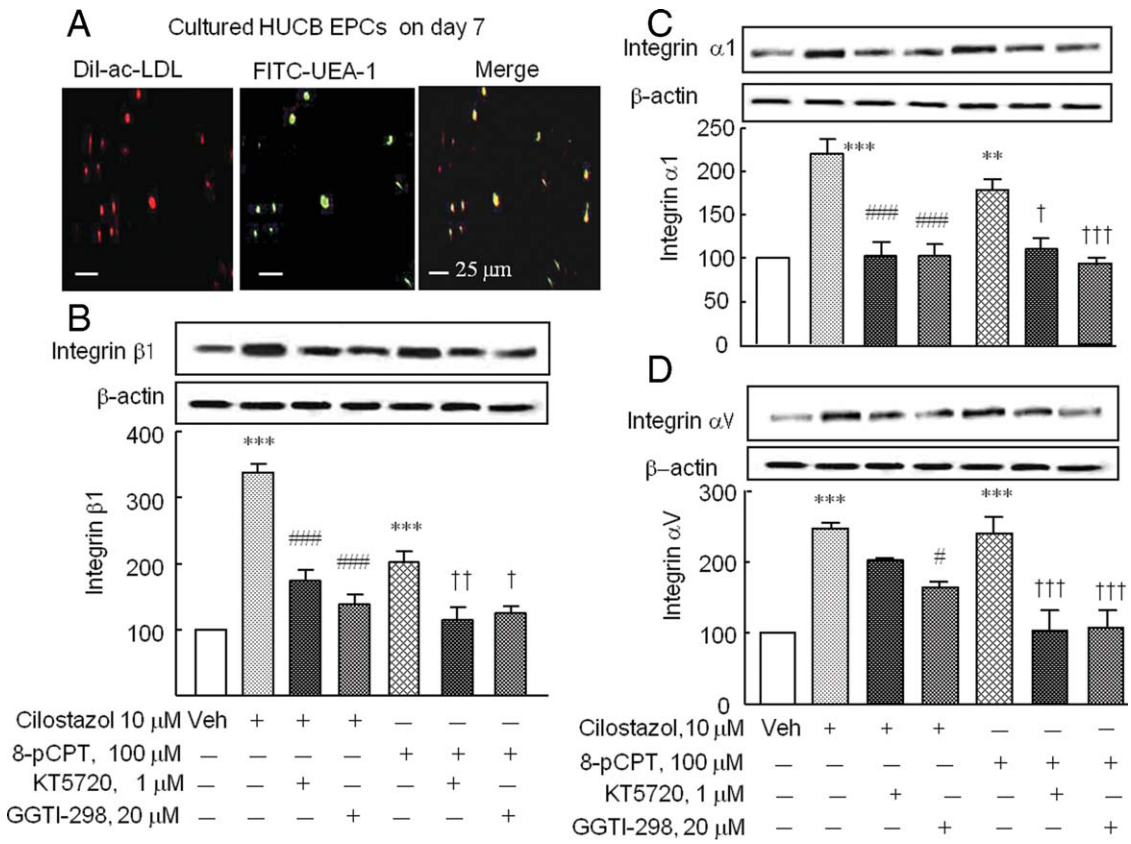

Fig. 1. **A:** Mononuclear cells (MNC) isolated from human umbilical cord blood (HUBC) were cultivated. On day 7, the phenotype of ex-vivo-cultivated EPCs was confirmed by double-positive immunostaining for the uptake of Dil-Ac-LDL and FITC-UEA-1 binding. Increased expression of integrin subunits β1 (**B**), α1 (**C**), and αV (**D**) of human EPCs by cilostazol (10 μM) and 8-pCPT (100 μM) without and with KT5720 (1 μM) and GGTI-298 (20 μM), respectively. Experimental protocols of C data are the same as those of D. Densitometric analyses are expressed as the mean ± SEM of four or five independent experiments. $^{**}P < 0.01$, $^{***}P < 0.001$ vs. Veh (vehicle); $^{\#}P < 0.05$, $^{\#\#\#}P < 0.001$ vs. 10 μM cilostazol; $\dagger P < 0.05$, $\dagger\dagger P < 0.01$, $\dagger\dagger\dagger P < 0.001$ vs. 100 μM 8-pCPT. Scale bar = 100 μm.

Activation of Epac1 and Rap1 GTP in the HUCB EPCs

Epac1, a guanine nucleotide exchange factor for the small GTPase known as Rap1, was significantly expressed in the HUCB EPCs. The stimulation of EPCs with cilostazol (3–30 μM) caused a concentration-dependent increase in Epac1 expression, as did 8-pCPT, a specific Epac activator (100 μM; Fig 3A). Treatment with either KT5720 (1 μM) or GGTI-298 (20 μM) alone had no effect on cilostazol stimulated-Epac1 expression (Fig. 3B).

Next, stimulation of Epac by cilostazol was investigated to determine whether it could increase the active GTP-bound form of Rap1 in the EPCs. Cilostazol increased Rap1 GTP expression with a maximum value of 10 μM of cilostazol (239% ± 20%, $P < 0.001$ vs. vehicle), as did 8-pCPT (100 and 200 μM; Fig. 3C). The cilostazol- and 8-pCPT-stimulated Rap1 GTP values were significantly suppressed by KT5720 (1 μM) and GGTI-298 (20 μM), respectively (Fig. 3D). These data indicate that cilostazol increased expression of functional Epac1 in the HUCB EPCs, as did 8-pCPT. In addition, PKA as well as Epac1 activated Rap1 in the progenitor cells.

Up-Regulation of p-CREB Expression by 8-pCPT and Increased Rap1 Expression by N^6-Benzoyl-cAMP

Next, whether p-CREB expression (as a marker for PKA) was increased by 8-pCPT, an activator of Epac, and then N^6-benzoyl-cAMP, a cAMP analog, which activates PKA but not Epac, could increase expression of Rap1 GTP and whether these factors were inhibited by both KT5720 and GGTI-298 were studied. Treatment with 8-pCPT (100 μM) significantly increased p-CREB expression to 154.8% ± 9.3% ($P < 0.001$); this was significantly inhibited by KT5720 and Rp-cAMPS (PKA inhibitors) and GGTI-298 (a selective Rap1 inhibitor; Fig. 4A). In addition, N^6-benzoyl-cAMP (100 μM) also caused a significant increase of Rap1 GTP expression (190.7% ± 6.5%, $P < 0.001$), as did 8-pCPT (100 μM; 193.4% ± 9.1%, $P < 0.001$), and the increased levels of Rap1 GTP were significantly suppressed by both Rp-cAMPS and GGTI-298, indicating cooperative action of the two pathways (Fig. 4B).

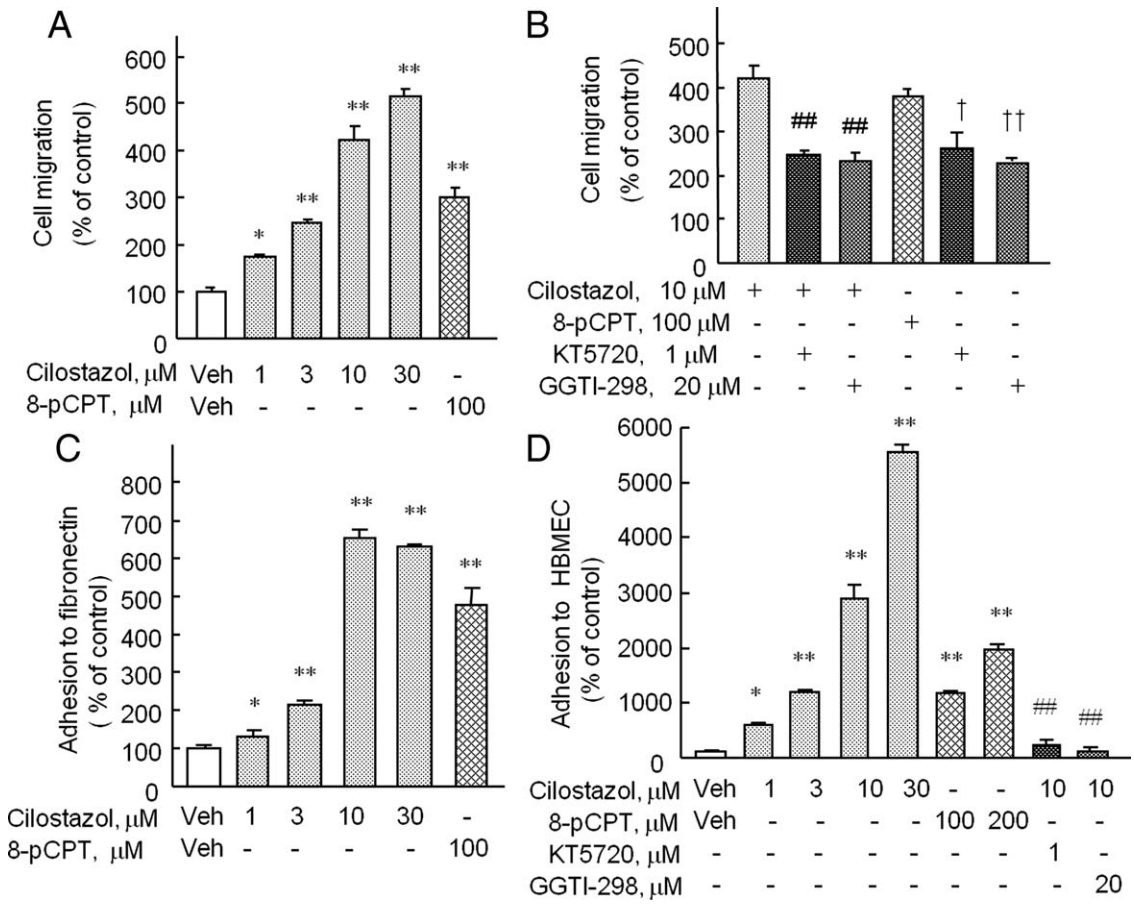

Fig. 2. **A:** Increased transcellular migration of the HUCB EPCs by cilostazol and 8-pCPT. **B:** Inhibitory effects of KT5720 and GGTI-298 on cilostazol- and 8-pCPT-stimulated migration of the EPCs. Effects of cilostazol and 8-pCPT on adhesion of EPCs to fibronectin (**C**) and to human brain microvascular endothelial cells (HBMEC; **D**) and the inhibitory effects of KT5720 (1 μM) and GGTI-298 (20 μM). Values are expressed as the mean ± SEM of three independent experiments. $*P < 0.05$, $**P < 0.01$ vs. Veh (vehicle); $^{\#\#}P < 0.01$ vs. cilostazol 10 μM; $\dagger P < 0.05$, $\dagger\dagger P < 0.01$ vs. 8-pCPT alone.

PKA Activation by 8-pCPT and N^6-Benzoyl-cAMP

Whether stimulation of Epac1 and Rap1 GTP, by cilostazol, could increase PKA activity in the HUCB EPCs was evaluated. The treatment with 8-pCPT (100 μM) stimulated PKA activity to 114.9 ± 3.0 PKA equivalents (ng) in a concentration-dependent manner; this was similar to the effects of cilostazol (112.4 ± 4.1 PKA equivalents, ng; Fig. 5A). Both 8-pCPT (100 μM)- and N^6-benzoyl-cAMP (100 μM)-stimulated PKA activities were significantly suppressed by KT5720 (1 μM), Rp-cAMPS (PKA inhibitors, 10 μM), and GGTI-298 (20 μM), as was cilostazol (10 μM; Fig. 5B,C). These findings implicate PKA-induced phosphorylation in Epac1 and Rap1 GTP activity stimulated by cilostazol in the HUCB EPCs.

Increased Homing of BM MNCs and Neovascularization in the Ischemic Injured Mouse Brain

By using immunofluorescence, confirmation of the in vivo relevance of cilostazol-mediated β1 integrin up-regulation was determined in the molecular layer of the hippocampus in the injured mouse brain after an ischemic insult. Cilostazol (30 mg/kg for 7 days) significantly increased the number of integrin β1-positve cells from 27.3 ± 1.5 cells/mm^2 to 73.8 ± 6.2 cells/mm^2, $P < 0.05$) in the molecular layer of the hippocampus (Fig. 6A). In addition, increased vascularization associated with up-regulation of homing of the BM MNCs to the molecular layer of the hippocampus was evaluated after cilostazol treatment for 7 and 14 days, after the ischemic event. When the CM-DiI-labeled BM MNCs were injected into the tail vein at 48 hr after transient forebrain ischemia, the cilostazol-treated mouse brain (for 7 days) showed a significant increase in the number of increased CM-DiI-labeled BM MNCs and vWF-positive cells (from vehicle, 1.83 ± 0.31 cells/mm^2 to 8.50 ± 0.76 cells/mm^2, $P < 0.001$) in the molecular layer of the hippocampus (Fig. 6B).

Fourteen days of treatment with cilostazol showed that the vWF staining was significantly increased with vWF-positive vessels within the molecular layer of the

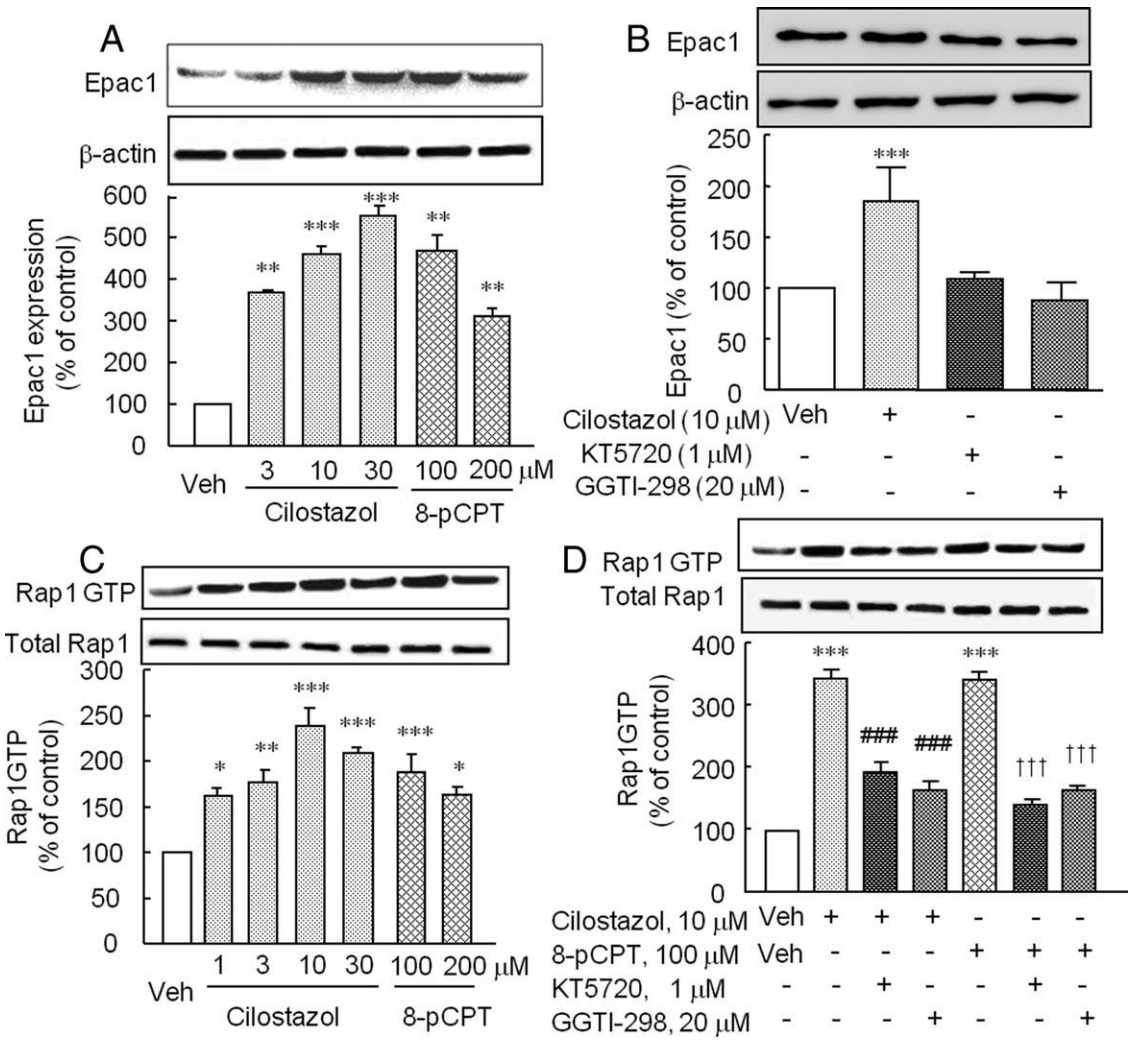

Fig. 3. **A:** Cilostazol- and 8-pCPT-stimulated Epac1 expression in the HUCB EPCs. EPCs were stimulated for 15 min in suspension either with cilostazol or 8-pCPT. **B:** Effects of KT5720 or GGTI-298 on Epac1 expression. **C:** Effects of cilostazol- and 8-pCPT on Rap1 GTP expression. **D:** Inhibition of cilostazol- and 8-pCPT-stimulated Rap1 GTP expression by KT5720 and GGTI-298. Densitometric analyses of Epac 1 and Rap1 GTP levels are expressed as the mean ± SEM of four or five independent experiments. $*P < 0.05$, $**P < 0.01$, $***P < 0.001$ vs. Veh (vehicle); $^{\#\#\#}P < 0.001$ vs. cilostazol; $\dagger\dagger\dagger P < 0.001$ vs. 8-pCPT.

hippocampus (708.7% ± 211.9%, $P < 0.05$ vs. vehicle group, 336.7% ± 93.5%) and dentate gyrus (556.7% ± 143.8%, $P < 0.05$ vs. vehicle group, 223.3% ± 110.1%) in the cilostazol-treated groups (Fig. 6C). The increased endothelial density indicated significant increase in the vascularization associated with cilostazol treatment.

DISCUSSION

In the present study, the implications of activation of both PKA and Epac1/Rap1 by cilostazol in integrin-dependent recruitment of progenitor cells were investigated in both in vitro and in vivo experiments. For the in vitro experiment with the HUCB EPCs, 1) expression of integrin subunits β1, α1, and αv was up-regulated in association with enhanced HUCB EPCs migration/adhesion to the fibronectin-coated plate and microvascular endothelial cells by treatment with cilostazol and 8-pCPT; this activity was significantly suppressed by KT5720 (a selective inhibitor of PKA) and GGTI-298 (a selective Rap1 inhibitor), respectively. 2) Cilostazol increased Epac1 expression and stimulated the active GTP-bound form of Rap1, as did 8-pCPT, a specific Epac1 activator, which was also significantly suppressed by both KT5720 and GGTI-298. 3) 8-pCPT (100 μM) significantly increased p-CREB expression, and N^6-benzoyl-cAMP (100 μM) was associated with a significant increase of Rap1 GTP expression. 4) Both 8-pCPT and N^6-benzoyl-cAMP significantly stimulated PKA activity, as did cilostazol, and they were significantly suppressed by KT5720, Rp-cAMPS (PKA inhibitors), and GGTI-298. For the in vivo experiment, 5) cilostazol (30 mg/kg/day, orally for 7 days) enhanced

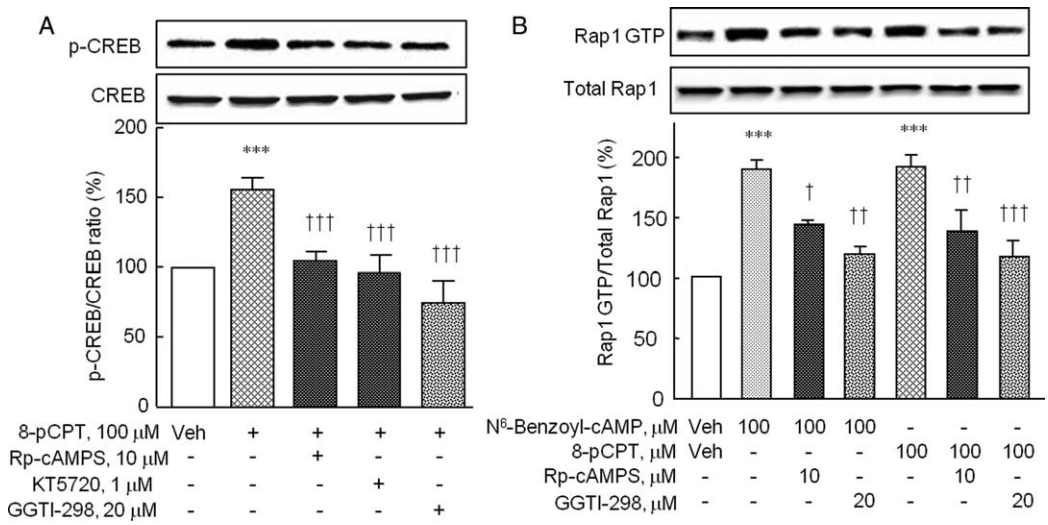

Fig. 4. Up-regulation of p-CREB expression by 8-pCPT (**A**) and increased Rap1 GTP expression by N^6-benzoyl-cAMP and 8-pCPT (**B**) in HUCB EPCs without and with KT5720 and Rp-cAMPS (inhibitors of PKA) and GGTI-298 (a selective Rap1 inhibitor). Values are expressed as the mean ± SEM of five or six experiments. $***P < 0.001$ vs. Veh (vehicle); $\dagger P < 0.05$, $\dagger\dagger P < 0.01$, $\dagger\dagger\dagger$ $P < 0.001$ vs. N^6-benzoyl-cAMP or 8-pCPT, respectively.

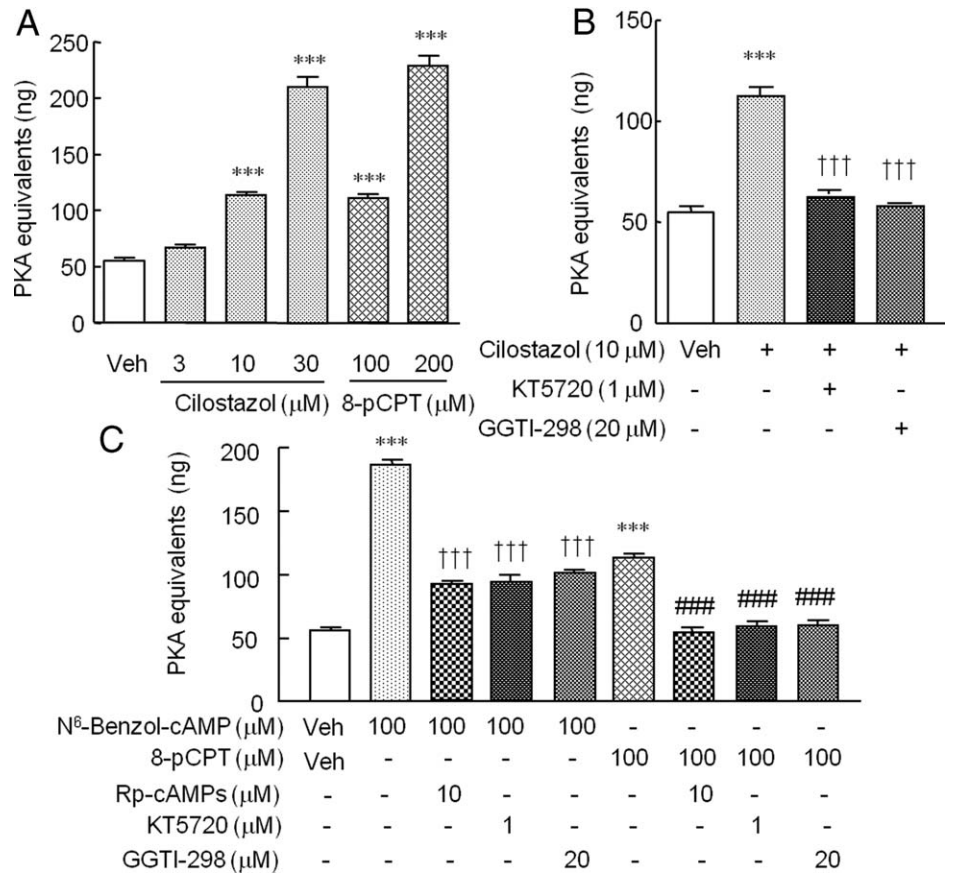

Fig. 5. **A:** Concentration-dependent increase in PKA activity by cilostazol and 8-pCPT in the HUCB EPCs. **B:** Effects of KT5720 and GGTI-298 on cilostazol-stimulated PKA activity. **C:** Effects of KT5720 and Rp-cAMPS and GGTI-298 on N^6-benzoyl-cAMP and 8-pCPT-stimulated PKA activity, respectively. Values are expressed as the mean ± SEM of three experiments in duplicate. $***P < 0.001$ vs. Veh (vehicle); $\dagger\dagger\dagger P < 0.001$ vs. cilostazol or N^6-benzoyl-cAMP; $^{\#\#\#}P < 0.001$ vs. 8-pCPT.

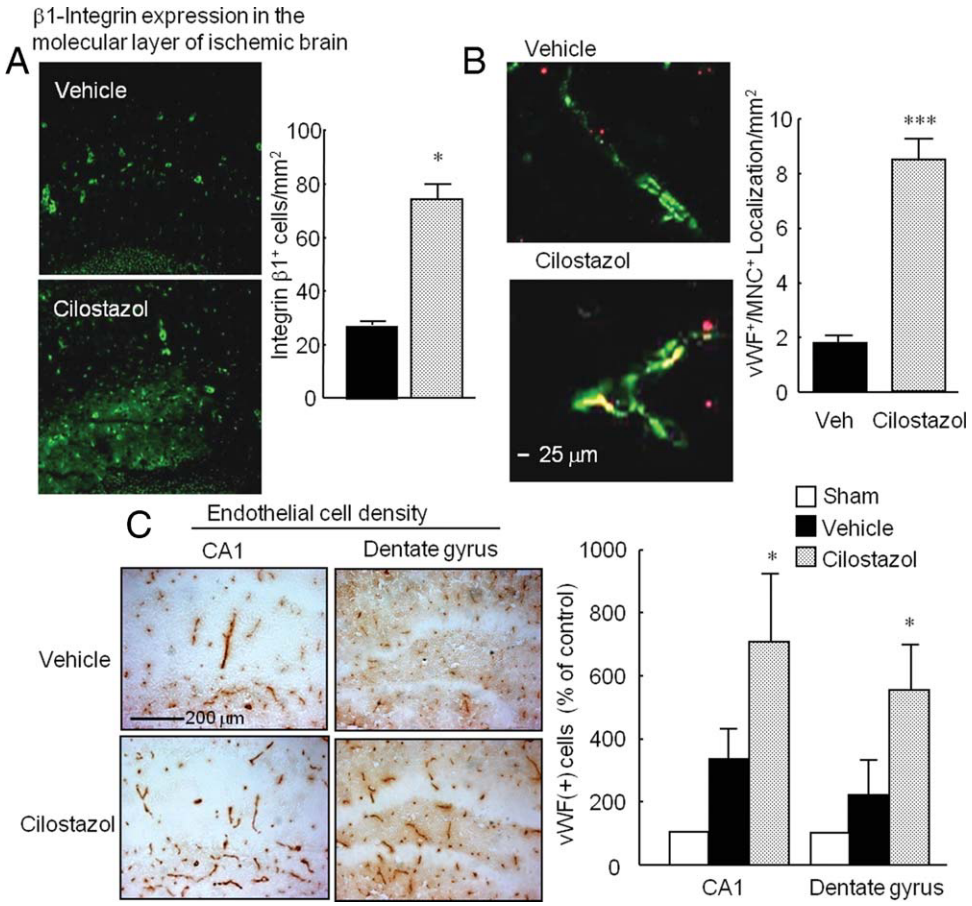

Fig. 6. **A:** Representative images of integrin β1-positive cells in the molecular layer of the hippocampus of mouse brain subjected to transient forebrain ischemia and the quantitative data. The mice received cilostazol (30 mg/kg/day, orally) for 7 days. **B:** Increased colocalization of vWF- and BM MNC-positive cells by cilostazol in the molecular layer of the hippocampus. Infused progenitor cells were identified as CM-DiI-labeled cells (red) and von Willebrand factor (vWF, a specific marker for endothelial cells) as the green fluorescence. Quantitative data of vWF^+/MNC^+ colocalization (cells/mm^2) are expressed as the mean ± SEM from six mice. $***P < 0.001$ vs. Veh (vehicle). **C:** Photographs showing endothelial cell densities stained for vWF in the hippocampus of cilostazol-treated mice 14 days after ischemia. Quantitative analysis of vWF-positive cells is expressed as the mean ± SEM (% of control) from five mice in each group. $*P < 0.05$ vs. vehicle.

the homing capability of the BM MNCs with enhanced expression of the integrin β1 subunit in the molecular layer of the hippocampus in the mouse brain after an ischemic insult. Finney et al. (2006) reported that EPCs derived from adult bone marrow can mediate neovasculogenesis in murine models of vascular injury; in addition, injection of either HUCB- or BM-derived EPCs was reported to result in significantly improved perfusion by 7 and 14 days after femoral artery ligation in mice with equivalent capillary densities. However, the amount of available EPCs from bone marrow is usually too limited for use in a variety of in vitro biochemical experiments; thus, in this study, HUCB EPCs were used for the in vitro experiment, and EPCs derived from BM MNCs were used for the in vivo study.

Cilostazol has recently been reported to exert protective effects against cognitive impairment and white matter lesions induced by chronic cerebral hypoperfusion in rats subjected to bilateral common carotid artery ligation (Lee et al., 2006). In addition, cilostazol has been reported to have dual beneficial effects: one the preservation of the CA1 hippocampal region, and the other promotion of the generation of immature migratory neuroblasts in the dentate gyrus by up-regulation of CREB phosphorylation after transient forebrain ischemia (Lee et al., 2009). Moreover, Shin et al. (2010) reported that cilostazol was associated with increased recruitment of EPCs, positive for Sca-1/VEGFR-2 in the bone marrow and circulating peripheral blood. This finding was explained as evidence of beneficial interfaces, in which both bone marrow-derived EPCs and several angioneurins, including BDNF and VEGF, influence neurogenesis in tissues after an ischemic injury.

Integrins are membrane receptors that mediate cell–cell or cell–matrix adhesion. Cell adhesion molecules such as integrin β1 have been suggested as the principal endothelial receptors for basal lamina components such as collagen and laminin (Haring et al., 1996) and have been

shown to play a crucial role in microvasculature reactions (del Zoppo and Milner, 2006). In the integrin family, $\alpha1\beta1$ and $\alpha2\beta1$ are the main fibrillar collagen receptors; they bind the same collagen ligands (Heino, 2000). Adhesion of EPCs to denuded vessels is mediated by vitronectin receptors (integrins $\alpha v\beta3$ and $\alpha v\beta5$) that are involved in reendothelialization of injured carotid arteries (Walter et al., 2002). The expression of various integrin subunits with cilostazol was evaluated in this study. Cilostazol (10 μM) and 8-pCPT (100 μM) up-regulated expression of integrin β1, α1, and αv; and they acted in a similar manner. Consistent with these findings, cilostazol significantly enhanced transcellular migration and adhesion of EPCs to the fibronectin-coated plate and microvascular endothelial cells, as did treatment with 8-pCPT.

Next, stimulation of Epac by cilostazol was studied to determine whether it could increase the active GTP-bound form of Rap1 and whether Epac1-Rap1 signals could regulate cAMP-dependent PKA, similarly to cilostazol in HUCB EPCs. The results showed that stimulation of the HUCB EPCs with cilostazol (3–30 μM) increased Epac1 expression and the level of the active GTP-bound forms of Rap1, as did 8-pCPT (100 μM). Cilostazol- and 8-pCPT-stimulated Rap1 GTP values were significantly suppressed by KT5720 and GGTI-298 (a potent and selective inhibitor of Rap1 processing; Kogut et al., 2007). These results suggest the involvement of PKA activity of 8-pCPT in progenitor cells.

The mechanism by which KT5720 can inhibit 8-pCPT-stimulated Rap1 activity is thought to be associated with PKA phosphorylation of Src at serine residue 17; this is required for activation of the small G protein known as Rap1 in NIH3T3 cells (Schmitt and Stork, 2002) and for nerve growth factor signaling in PC12 cells (Obara et al., 2004). Hochbaum et al. (2008) reported that, although 8-pMeOPT-2′-O-Me-cAMP does not trigger a proliferative response, it significantly potentiates the activity of the PKA-specific analog N^6-benzoyl-cAMP (Christensen et al., 2003), which is due to the cooperation of the cAMP effector pathways, Epac and PKA. One could envision various scenarios with regard to the way in which KT5720, a PKA inhibitor, inhibits 8-pCPT-stimulated integrin expression and migration/adhesion of EPCs. Rap1b, a substrate for Epac, and PKA have been reported to play an essential role in cAMP-mediated cell migration and adhesion in cellular (Ribeiro-Neto et al., 2002) and mouse models (Ribeiro-Neto et al., 2004). The findings from such studies suggest that inhibition of 8-pCPT-stimulated Rap1 activity by KT5720 could be ascribed to its inhibitory action on Rap1 phosphorylation by PKA. Consistent with the results of these previous reports, the results of this study showed that p-CREB expression (as a marker of PKA) was increased by 8-pCPT, an activator of Epac, and N^6-benzoyl-cAMP, a cyclic AMP analog that activates PKA but not Epac (Christensen et al., 2003), which could also increase expression of Rap1

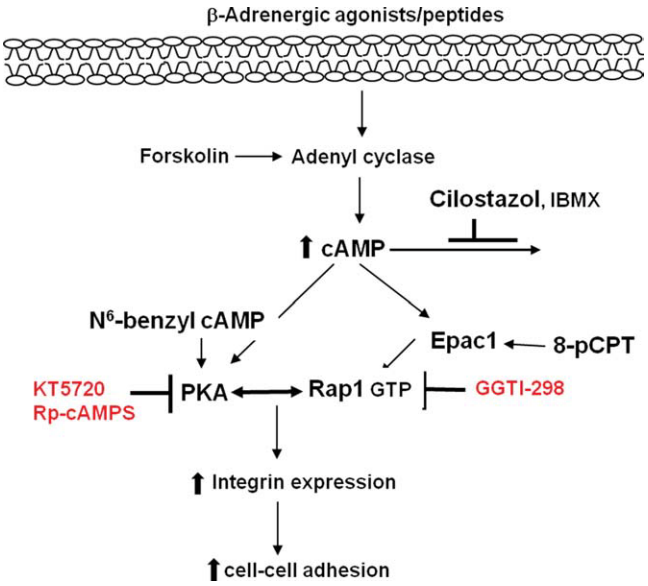

Fig. 7. Proposed mechanism(s) by which cilostazol increases integrin expression in endothelial progenitor cells through activation of cAMP-dependent protein kinase (PKA), in synergy with Epac1/Rap1 GTP. PDE, phosphodiesterase; IBMX, 3-isobutyl-1-methyl xanthine. [Color figure can be viewed in the online issue, which is available at wileyonlinelibrary.com.]

GTP; these factors were significantly inhibited by both KT5720 and GGTI-298, indicating that two cAMP effector enzymes, PKA and Epac1, cooperatively enhance migration and adhesion of EPCs with increased integrin expression.

However, the molecular mechanism of the PKA-dependent Rap1 phosphorylation remains unknown. Therefore, PKA activity was evaluated. Treatment with 8-pCPT significantly stimulated PKA activity in a concentration-dependent manner; this was similar to cilostazol. Both 8-pCPT- and N^6-benzoyl-cAMP-stimulated PKA activities were significantly suppressed by KT5720 and Rp-cAMPS and GGTI-298, as was cilostazol. These results provide evidence to support PKA-induced phosphorylation in the action of Epac1 and Rap1 GTP, stimulated by cilostazol in the HUCB EPCs (Fig. 7).

Carmona et al. (2008) demonstrated that stimulation with 8-pCPT, an Epac activator, enhanced homing of intravenously injected human peripheral blood-derived EPCs to ischemic limbs in a murine model of hind limb ischemia. Consistent with this finding, the results from the in vivo experiment of this study showed that cilostazol (30 mg/kg/day for 7 days) up-regulated homing of the BM MNCs with increased capillary density, accompanied by enhanced expression of the integrin β1 subunit in the molecular layer of the hippocampal area of the mouse brain subjected to 20 min of transient forebrain ischemia.

Taken together, the results of this study show that cilostazol stimulated migration and adhesion of EPCs; in addition, enhanced integrin expression through

cAMP-PKA activation was demonstrated, in concert with Epac/Rap1 GTP activation. This activity resulted in increased neovascularization.

REFERENCES

Asahara T, Murohara T, Sullivan A, Silver M, van der Zee R, Li T, Witzenbichler B, Schatteman G, Isner JM. 1997. Isolation of putative progenitor endothelial cells for angiogenesis. Science 275:964–967.

Bos JL. 2005. Linking Rap to cell adhesion. Curr Opin Cell Biol 17:123–128.

Burggraf D, Trinkl A, Burk J, Martens HK, Dichgans M, Hamann GF. 2008. Vascular integrin immunoreactivity is selectively lost on capillaries during rat focal cerebral ischemia and reperfusion. Brain Res 1189:189–197.

Carmona G, Chavakis E, Koehl U, Zeiher AM, Dimmeler S. 2008. Activation of Epac stimulates integrin-dependent homing of progenitor cells. Blood 111:2640–2646.

Christensen AE, Selheim F, de Rooij J, Dremier S, Schwede F, Dao KK, Martinez A, Maenhaut C, Bos JL, Genieser HG, Døskeland SO. 2003. cAMP analog mapping of Epac1 and cAMP kinase. Discriminating analogs demonstrate that Epac and cAMP kinase act synergistically to promote PC-12 cell neurite extension. J Biol Chem 278:35394–35402.

de Rooij J, Zwartkruis FJ, Verheijen MH, Cool RH, Nijman SM, Wittinghofer A, Bos JL. 1998. Epac is a Rap1 guanine nucleotide-exchange factor directly activated by cyclic AMP. Nature 396:474–477.

del Zoppo GJ, Milner R. 2006. Integrin–matrix interactions in the cerebral microvasculature. Arterioscler Thromb Vasc Biol 26:1966–1975.

Finney MR, Greco NJ, Haynesworth SE, Martin JM, Hedrick DP, Swan JZ, Winter DG, Kadereit S, Joseph ME, Fu P, Pompili VJ, Laughlin MJ. 2006. Direct comparison of umbilical cord blood vs. bone marrow-derived endothelial precursor cells in mediating neovascularization in response to vascular ischemia. Biol Blood Marrow Transplant 12:585–593.

Haring HP, Akamine BS, Habermann R, Koziol JA, Del Zoppo GJ. 1996. Distribution of integrin-like immunoreactivity on primate brain microvasculature. J Neuropathol Exp Neurol 55:236–245.

Heino J. 2000. The collagen receptor integrins have distinct ligand recognition and signaling functions. Matrix Biol 19:319–323.

Hochbaum D, Hong K, Barila G, Ribeiro-Neto F, Altschuler DL. 2008. Epac, in synergy with cAMP-dependent protein kinase (PKA), is required for cAMP-mediated mitogenesis. J Biol Chem 283:4464–4468.

Jin H, Aiyer A, Su J, Borgstrom P, Stupack D, Friedlander M, Varner J. 2006. A homing mechanism for bone marrow-derived progenitor cell recruitment to the neovasculature. J Clin Invest 116:652–662.

Kawasaki H, Springett GM, Mochizuki N, Toki S, Nakaya M, Matsuda M, Housman DE, Graybiel AM. 1998. A family of cAMP-binding proteins that directly activate Rap1. Science 282:2275–2279.

Kimura Y, Tani T, Kanbe T, Watanabe K. 1985. Effect of cilostazol on platelet aggregation and experimental thrombosis. Arzneimittelforschung 35:1144–1149.

Kogut MH, Genovese KJ, He H. 2007. Flagellin and lipopolysaccharide stimulate the MEK-ERK signaling pathway in chicken heterophils through differential activation of the small GTPases, Ras and Rap1. Mol Immunol 44:1729–1736.

Kooistra MR, Dube N, Bos JL. 2007. Rap1: a key regulator in cell–cell junction formation. J Cell Sci 120:17–22.

Lee JH, Park SY, Shin YW, Hong KW, Kim CD, Sung SM, Kim KY, Lee WS. 2006. Neuroprotection by cilostazol, a phosphodiesterase type 3 inhibitor, against apoptotic white matter changes in rat after chronic cerebral hypoperfusion. Brain Res 1082:182–191.

Lee JH, Park SY, Shin HK, Kim CD, Lee WS, Hong KW. 2008. Protective effects of cilostazol against transient focal cerebral ischemia and chronic cerebral hypoperfusion injury. CNS Neurosci Ther 14:143–152.

Lee JH, Shin HK, Park SY, Kim CD, Lee WS, Hong KW. 2009. Cilostazol preserves CA1 hippocampus and enhances generation of immature neuroblasts in dentate gyrus after transient forebrain ischemia in rats. Exp Neurol 215:87–94.

Lorenowicz MJ, Fernandez-Borja M, Kooistra MRH, Bos JL, Hordijk PL. 2008. PKA and Epac1 regulate endothelial integrity and migration through parallel and independent pathways. Eur J Cell Biol 87:779–792.

Murohara T. 2001. Therapeutic vasculogenesis using human cord blood-derived endothelial progenitors. Trends Cardiovasc Med 11:303–307.

Obara Y, Labudda K, Dillon TJ, Stork PJ. 2004. PKA phosphorylation of Src mediates Rap1 activation in NGF and cAMP signaling in PC12 cells. J Cell Sci 117:6085–6094.

Rangarajan S, Enserink JM, Kuiperij HB, de Rooij J, Price LS, Schwede F, Bos JL. 2003. Cyclic AMP induces integrin-mediated cell adhesion through Epac and Rap1 upon stimulation of the beta 2-adrenergic receptor. J Cell Biol 160:487–493.

Ribeiro-Neto F, Urbani J, Lemee N, Lou L, Altschuler DL. 2002. On the mitogenic properties of Rap1b: cAMP-induced G_1/S entry requires activated and phosphorylated Rap1b. Proc Natl Acad Sci U S A 99:5418–5423.

Ribeiro-Neto F, Leon A, Urbani-Brocard J, Lou L, Nyska A, Altschuler DL. 2004. cAMP-dependent oncogenic action of Rap1b in the thyroid gland. J Biol Chem 279:46868–46875.

Roscioni SS, Elzinga CRS, Schmidt M. 2008. Epac: effectors and biological functions. Naunyn Schmiedebergs Arch Pharmacol 377:345–357.

Schmitt JM, Stork PJ. 2002. PKA phosphorylation of Src mediates cAMP's inhibition of cell growth via Rap1. Mol Cell 9:85–94.

Shin HK, Lee HR, Lee DH, Hong KW, Lee JH, Park SY, Lee SJ, Lee JS, Lee WS, Rhim BY, Kim CD. 2010. Cilostazol enhances neovascularization in the mouse hippocampal area subjected to transient global ischemia. J Neurosc Res 88:2228–2238.

Urbich C, Dimmeler S. 2004. Endothelial progenitor cells: characterization and role in vascular biology. Circ Res 95:343–353.

Vajkoczy P, Blum S, Lamparter M, Mailhammer R, Erber R, Engelhardt B, Vestweber D, Hatzopoulos AK. 2003. Multistep nature of microvascular recruitment of ex vivo-expanded embryonic endothelial progenitor cells during tumor angiogenesis. J Exp Med 197:1755–1765.

Vasa M, Fichtlscherer S, Aicher A, Adler K, Urbich C, Martin H, Zeiher AM, Dimmeler S. 2001. Number and migratory activity of circulating endothelial progenitor cells inversely correlate with risk factors for coronary artery disease. Circ Res 89:E1–E7.

Walter DH, Rittig K, Bahlmann FH, Kirchmair R, Silver M, Murayama T, Nishimura H, Losordo DW, Asahara T, Isner JM. 2002. Statin therapy accelerates reendothelialization: a novel effect involving mobilization and incorporation of bone marrow-derived endothelial progenitor cells. Circulation 105:3017–3024.

Wu Y, Ip JE, Huang J, Zhang L, Matsushita K, Liew CC, Pratt RE, Dzau VJ. 2006. Essential role of ICAM-1/CD18 in mediating EPC recruitment, angiogenesis, and repair to the infarcted myocardium. Circ Res 99:315–322.